NASA/TM—2007-214978 ARL–TR–4126

Experimental Investigation of Rotating Stall in a Research Multistage Axial Compressor

Jan Lepicovsky
ASRC Aerospace Corporation, Cleveland, Ohio

Edward P. Braunscheidel
Glenn Research Center, Cleveland, Ohio

Gerard E. Welch
U.S. Army Research Laboratory, Glenn Research Center, Cleveland, Ohio

August 2007

NASA STI Program . . . in Profile

Since its founding, NASA has been dedicated to the advancement of aeronautics and space science. The NASA Scientific and Technical Information (STI) program plays a key part in helping NASA maintain this important role.

The NASA STI Program operates under the auspices of the Agency Chief Information Officer. It collects, organizes, provides for archiving, and disseminates NASA's STI. The NASA STI program provides access to the NASA Aeronautics and Space Database and its public interface, the NASA Technical Reports Server, thus providing one of the largest collections of aeronautical and space science STI in the world. Results are published in both non-NASA channels and by NASA in the NASA STI Report Series, which includes the following report types:

- TECHNICAL PUBLICATION. Reports of completed research or a major significant phase of research that present the results of NASA programs and include extensive data or theoretical analysis. Includes compilations of significant scientific and technical data and information deemed to be of continuing reference value. NASA counterpart of peer-reviewed formal professional papers but has less stringent limitations on manuscript length and extent of graphic presentations.

- TECHNICAL MEMORANDUM. Scientific and technical findings that are preliminary or of specialized interest, e.g., quick release reports, working papers, and bibliographies that contain minimal annotation. Does not contain extensive analysis.

- CONTRACTOR REPORT. Scientific and technical findings by NASA-sponsored contractors and grantees.

- CONFERENCE PUBLICATION. Collected papers from scientific and technical conferences, symposia, seminars, or other meetings sponsored or cosponsored by NASA.

- SPECIAL PUBLICATION. Scientific, technical, or historical information from NASA programs, projects, and missions, often concerned with subjects having substantial public interest.

- TECHNICAL TRANSLATION. English-language translations of foreign scientific and technical material pertinent to NASA's mission.

Specialized services also include creating custom thesauri, building customized databases, organizing and publishing research results.

For more information about the NASA STI program, see the following:

- Access the NASA STI program home page at *http://www.sti.nasa.gov*

- E-mail your question via the Internet to *help@sti.nasa.gov*

- Fax your question to the NASA STI Help Desk at 301–621–0134

- Telephone the NASA STI Help Desk at 301–621–0390

- Write to:
  NASA Center for AeroSpace Information (CASI)
  7115 Standard Drive
  Hanover, MD 21076–1320

NASA/TM—2007-214978 ARL–TR–4126

Experimental Investigation of Rotating Stall in a Research Multistage Axial Compressor

Jan Lepicovsky
ASRC Aerospace Corporation, Cleveland, Ohio

Edward P. Braunscheidel
Glenn Research Center, Cleveland, Ohio

Gerard E. Welch
U.S. Army Research Laboratory, Glenn Research Center, Cleveland, Ohio

Prepared for the
18th ISABE Conference (ISABE 2007)
sponsored by the International Society for Air Breathing Engines
Beijing, China, September 2–7, 2007

National Aeronautics and
Space Administration

Glenn Research Center
Cleveland, Ohio 44135

August 2007

Acknowledgments

The work was sponsored by the NASA Glenn Research Center under the Intelligent Propulsion Systems Foundation Technologies by Dr. C. R. Mercer. The first author would like to thank Mr. J. P. Veres, chief of the GRC Compressor Branch, for his support and permission to publish the results of this study. Many useful discussions with Dr. M. D. Hathaway of Army Research Laboratory, and significant help from Ms. E. L. Parrott and Mr. R. Torres, both of NASA GRC, are also gratefully acknowledged.

This work was sponsored by the Fundamental Aeronautics Program at the NASA Glenn Research Center.

Level of Review: This material has been technically reviewed by technical management.

Available from

NASA Center for Aerospace Information
7115 Standard Drive
Hanover, MD 21076–1320

National Technical Information Service
5285 Port Royal Road
Springfield, VA 22161

Available electronically at http://gltrs.grc.nasa.gov

Experimental Investigation of Rotating Stall in a Research Multistage Axial Compressor

Jan Lepicovsky
ASRC Aerospace Corporation
Cleveland, Ohio 44135

Edward P. Braunscheidel
National Aeronautics and Space Administration
Glenn Research Center
Cleveland, Ohio 44135

Gerard E. Welch
U.S. Army Research Laboratory
Glenn Research Center
Cleveland, Ohio 44135

Abstract

A collection of experimental data acquired in the NASA low-speed multistage axial compressor while operated in rotating stall is presented in this paper. The compressor was instrumented with high-response wall pressure modules and a static pressure disc probe for in-flow measurement, and a split-fiber probe for simultaneous measurements of velocity magnitude and flow direction. The data acquired to-date have indicated that a single fully developed stall cell rotates about the flow annulus at *50.6%* of the rotor speed. The stall phenomenon is substantially periodic at a fixed frequency of *8.29 Hz*. It was determined that the rotating stall cell extends throughout the entire compressor, primarily in the axial direction. Spanwise distributions of the instantaneous absolute flow angle, axial and tangential velocity components, and static pressure acquired behind the first rotor are presented in the form of contour plots to visualize different patterns in the outer (mid-span to casing) and inner (hub to mid-span) flow annuli during rotating stall. In most of the cases observed, the rotating stall started with a single cell. On occasion, rotating stall started with two emerging stall cells. The root cause of the variable stall cell count is unknown, but is not attributed to operating procedures.

Nomenclature

V_X	$[m.s^{-1}]$	axial velocity component
V_θ	$[m.s^{-1}]$	tangential velocity component
C_X	$[1]$	axial velocity coefficient $[= V_X/U_T]$
C_θ	$[1]$	tangential velocity coefficient $[= V_\theta/U_T]$
C_{PS}	$[1]$	static pressure coefficient $[= (p_S - p_{AMB}) / (0.5\ \rho\ U_T^2)]$
h	$[1]$	dimensionless blade span from hub
N_{ROT}	$[1]$	rotor revolution
p_{AMB}	$[kPa]$	ambient pressure
p_S	$[kPa]$	in-flow static pressure
$p_{S,W}$	$[kPa]$	wall (casing) static pressure
t	$[s]$	time
U_T	$[m.s^{-1}]$	blade tip velocity
$V_{X,IN}$	$[m.s^{-1}]$	inlet average axial velocity
α	$[dg]$	absolute flow angle, relative to axial
Φ	$[1]$	flow coefficient $[= V_{X,IN}/U_{BT}]$
ρ	$[kg.m^{-3}]$	air density
τ_{SCP}	$[1]$	normalized period of stall cell passage
Ω	$[1]$	fraction of circumference

Introduction

Rotating stall in axial fans and compressors has been the subject of extensive research (Refs. 1 through 8). The consequences of a rotating stall can include rapid deterioration of engine performance (and ultimately engine surge) and fatigue-failure of a component due to prolonged stall cell buffeting. While compression system stability boundaries are implicitly avoided by incorporating margins into the component design, the continued push for higher aerodynamic loading levels and efficiency and wide-operability impels continued research related to rotating stall, its inception and avoidance.

Numerous publications document research efforts related to inception of rotating stall in single-stage and multistage compressors (Refs. 6 through 8) and to the flow field associated with fully developed stall cells (Refs. 4, 5 and 9). The present effort aims to contribute to this body of knowledge by documentation of experimental measurements and findings related to fully developed rotating stall cells obtained in the NASA low-speed multistage (4.5 stage) axial compressor.

Test Facility and Instrumentation

The NASA Low Speed Axial Compressor (LSAC) is described in detail in Refs. 10 through 12. The research compressor comprises an inlet guide vane followed by four geometrically identical axial stages (rotors and stators). The LSAC was modeled

after the GE Low-Speed Research Compressor (Ref. 13). Details of the LSAC are provided in Table 1. The compressor can be configured with a casing treatment over the first rotor; however, in the present work the rig was configured without casing treatment, that is with a smooth, solid casing. The compressor was operated during this entire investigation at a constant physical speed of *984 ± 1 rpm*.

Table 1. Compressor basic parameters.

		IGV	RBR	SVR
Number of rows		1	4	4
No. of blades		52	39	52
Hub diameter	m	0.976	0.976	0.976
Case diameter	m	1.219	1.219	1.219
Chord at midspan	mm	67	102	94
Settig angle at midspan	dg	3	51	31
Aspect ratio		1.820	1.195	1.297
Solidity at midspan		1.010	1.154	1.418
Tip clearance (% chord)	%	0	1.02	0
Axial gap (% RBR chord)	%	109.8	24.9	24.9
Design flow coefficient		0.395		
Design press. rise coeff.		0.500		
Design reaction (%)		62.8		
Stalling flow coefficient		0.345		
Stall. press. rise coeff.		0.560		
Design tip speed	$m.s^{-1}$	61.0		
Engine order, 100% speed	Hz	15.93		

The compressor blade layout and measurement stations for unsteady flow parameters are shown in Fig. 1. A flush-mounted wall plug containing a high-response pressure transducer measured instantaneous static pressure at the casing wall near the IGV trailing edge at a mid pitch location, measurement port S05A. The wall plug was kept at this port for all the measurements reported herein. Its signal served as the synchronization signal, and as a base for conditional sampling for all the other probes employed during this investigation. High-response wall pressure plugs, and thermo-anemometric and high-response static pressure probes were inserted one by one in the flow via ports *S15A*, *S15B*, *S35A*, *S35B*, *S40A*, and *S40B* to measure the flow pattern during rotating stall. The remaining ports, *S10B*, *S22A*, *S23A*, *S23B*, and *S24A*, were used for high-response wall static pressure measurements only.

The unsteady instrumentation, thermo-anemometric probe (split-fiber probe), and in-house designed and fabricated static pressure probe were described in detail in Ref. 9. Data reduction methods for decomposition of split-fiber probe data into velocity and flow direction components were given in Refs. 9, 14, and 15. The method of phase-locked ensemble averaging, including generation of ensemble base, was described in detail in Ref. 9.

In order to protect the sensitive unsteady pressure transducers used for the wall static pressure measurements against damage, and to ease frequent swapping of the transducers amongst individual ports, the transducers were built into modules that fit the internal diameter of the access ports. A schematic view of this module is shown in Fig. 2, and a photograph of an inserted module taken from inside the compressor is shown in Fig. 3. As seen here, the module was also furnished with a conventional static tap in order to verify the time averages of the high-response pressure transducers. It should be emphasized here that the steady state static pressure readings were not used for in-situ transducer calibration, but merely used for comparison with averages of measured unsteady pressures over a selected time period. All miniature pressure transducers (pressure range of *±7 kPa*, *±1 psig*) were carefully calibrated in an external facility, and eventual zero drift was compensated for by recording zero values before and after each test run. A view of four wall pressure transducer modules mounted in ports *S22A*, *S23A*, *S23B*, and *S24A* is shown in Fig. 4.

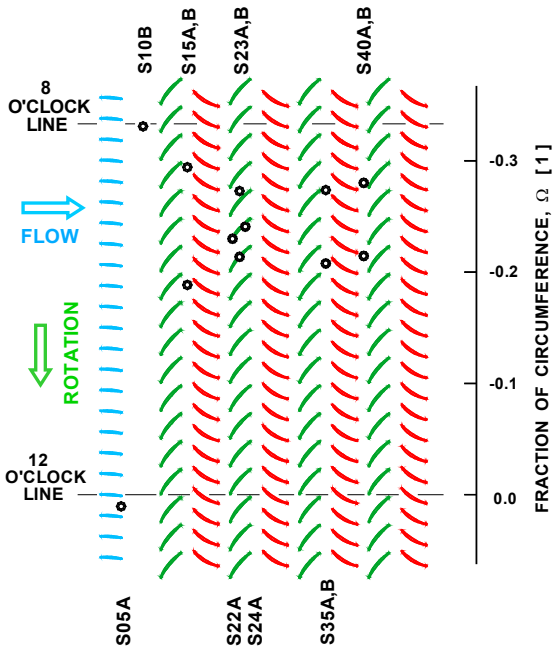

Figure 1. Compressor blading and layout of measurement ports.

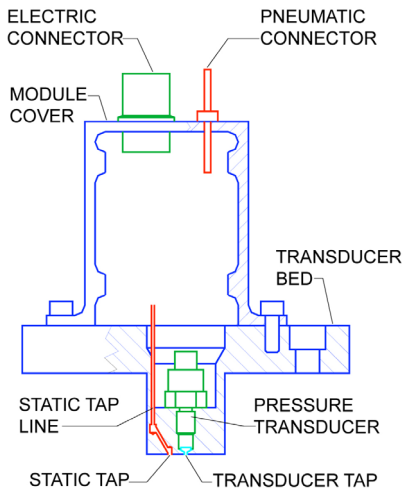

Figure 2. Transducer module for wall static pressure measurement.

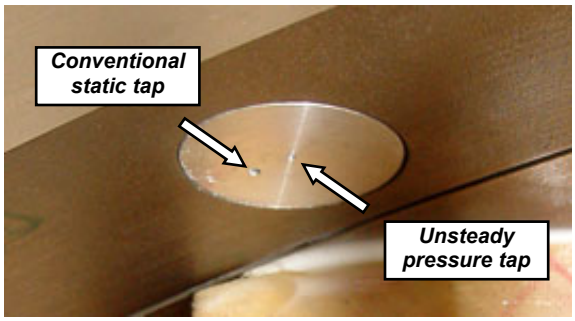

Figure 3. Wall static pressure probe mounted in the casing.

Figure 4. Four pressure transducer modules mounted on a compressor shroud.

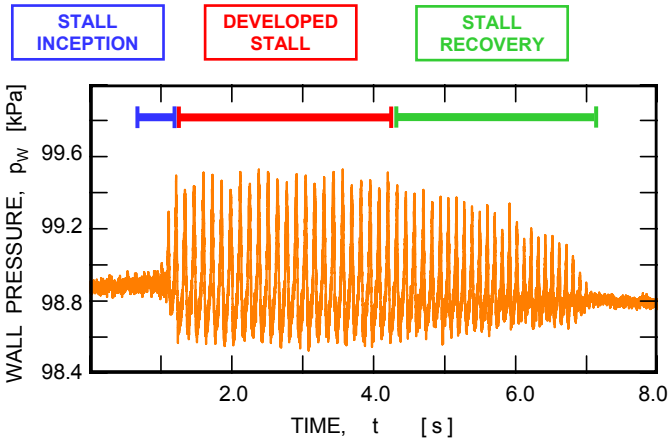

Figure 5. Phases of rotating stall regime.

Regime of Rotating Stall

Rotating stall is an unsteady, nonaxisymmetric flow phenomenon which can be induced as a fan or compressor is throttled beyond its stability boundary. To observe transients from a near-stall operating point into the rotating stall regime a consistent throttling procedure was followed. The throttling valve was closed at a constant rate starting from a flow coefficient of $\Phi = 0.35$, and once the rotating stall was detected, the valve motion was stopped and immediately reversed. The entire procedure lasted from *6 s* to *8 s* (i.e., *95* to *125* rotor revolutions). A response of the *S05A* pressure transducer to a transient from a stable pre-stall operating condition, to operation in rotating stall, and back is shown in Fig. 5 (Ref. 9). Three distinct phases of the rotating stall regime can be identified as indicated in the picture: stall inception, developed stall, and stall recovery. For measurements in the developed stall regime, the throttling valve was closed to a constant throttle position so as to establish a 'stable' rotating stall until the probe traversing along the blade span was completed (about *15* minutes). Data segments *10 s* long were taken at each probe position to acquire *80* stall cell passings.

Each test day started with measurements of speed line characteristics based on high-response casing static pressures. Casing static pressures recorded at select measurement stations for the design speed and developed rotating stall point are shown in Fig. 6. The plotted data were generated during the post-processing by averaging over a period of *4 s* (*32* stall cells). The rotating stall causes a sudden drop in pressure throughout the compressor as can be seen in the compressor characteristics shown in Fig. 6. The figure presents data taken from five ports along the compressor shroud. The red symbols shown in Fig. 6 correspond to the fully developed rotating stall (i.e., the stable rotating stall for the minimum setting of the throttling valve). The detailed flow field measurements reported in this paper were acquired for operation during this fully developed stall. The ratio of stall cell rotational speed to the rotor speed was fairly constant at an average value of *0.506*. A short discussion about transients from the last pre-stall operating condition into the rotating stall regime is presented at the end of this paper.

Axial Extent of a Rotating Stall Cell

It was desirable to simultaneously record wall pressure fluctuations at all twelve ports available on the compressor shroud to gain a comprehensive picture of the rotating stall pattern. However, due to the probe and recording hardware limitations, data from six ports only were recorded at a time, and the tests were repeated several times to cover all measurement stations, always overlapping some of the ports to assure repeatability of the acquired data. As seen in Fig. 1, the access ports were not arranged along an axial line but were scattered in the left half of the compressor shroud (between 8 and 12 o'clock). This layout was dictated by mechanical restrictions on the

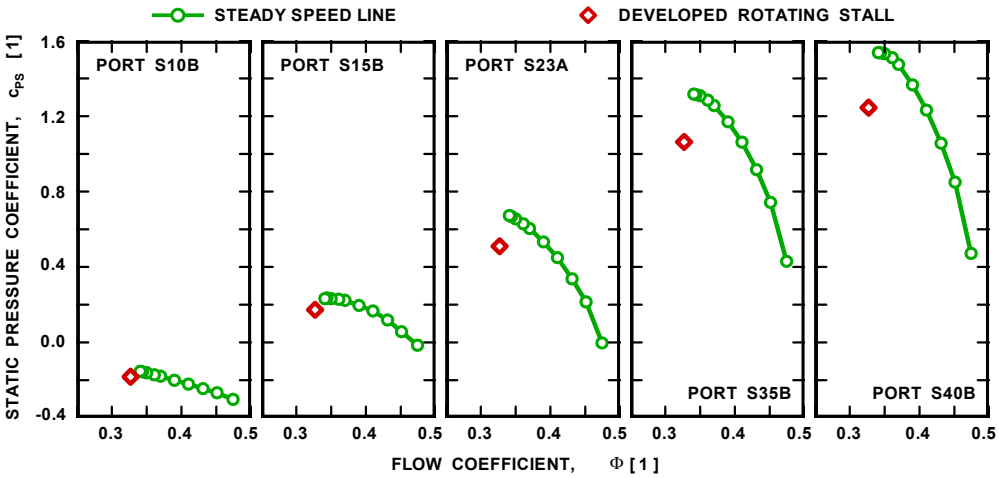

Figure 6. Casing static pressures measured for the design speed line and at the developed rotating stall point.

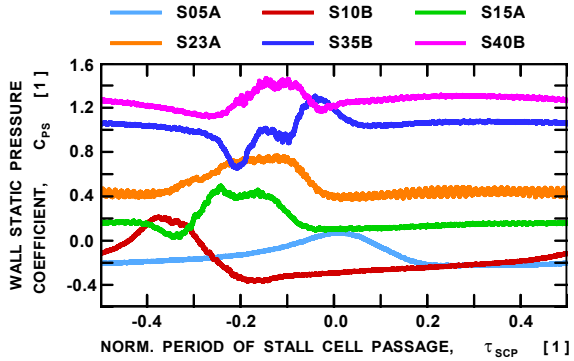

Figure 7. Unsteady pressures recorded on compressor casing.

compressor shroud. Consequently, a rotating stall cell did not pass the measurement stations simultaneously but rather with a time delay which was proportional to the rotational speed of the stall cell and the angular position of a given access port.

Traces of pressure data from six ports, as recorded, are presented in Fig. 7. The increased pressure regions on each trace indicate passage of the rotating stall cell, and its circumferential location reflects the angular position of the particular pressure port. The pressure distributions depicted are results of ensemble averaging phase-locked with the rotational speed of a stall cell recorded at port *S05A*. The ensemble averages were calculated from *80* passings of the rotating stall cell. The applied methodology of phase-locked ensemble averaging was described in detail in Ref. 9.

The LSAC data acquired to-date have indicated that the developed rotating stall is substantially periodic at a fixed frequency of *8.29 Hz* with the maximum variation within *±3.6%* (Ref. 9). Therefore, knowing the angular position of a given probe, the pressure signal can be shifted in the time-domain to coincide with the instant of the rotating cell passage by the master pressure measurement port (*S05A* in this case), thus effectively aligning all pressure ports axially at a fixed angular position (close to 12 o'clock). Results of this procedure, for all measurement ports and all wall pressure probes used, are shown in Fig. 8. The figure

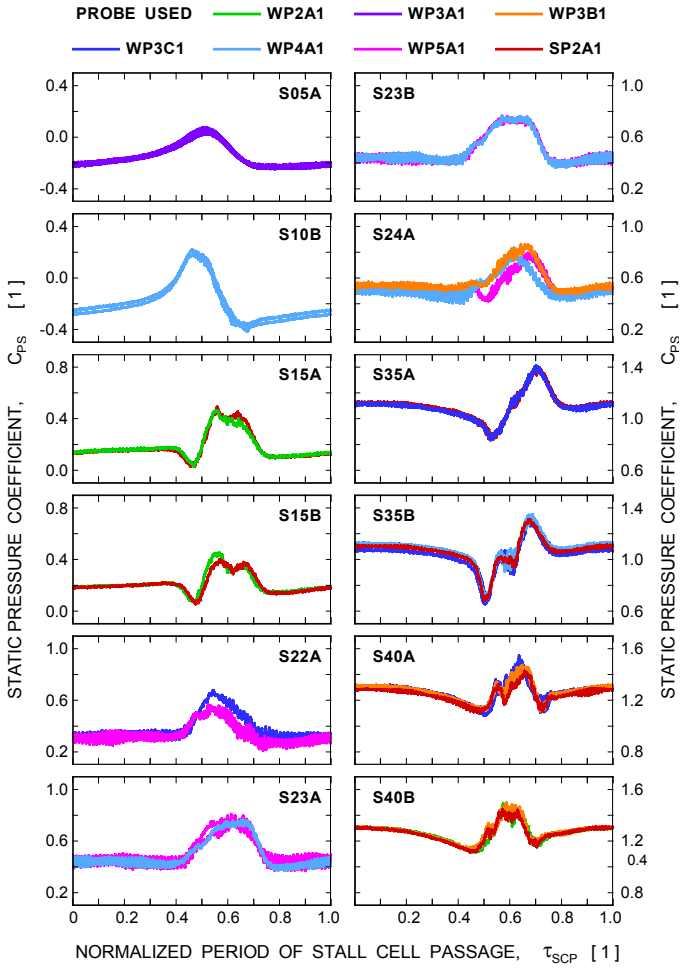

Figure 8. Unsteady pressure traces from ports along the casing aligned with angular position of port S05A (close to 12 o'clock line).

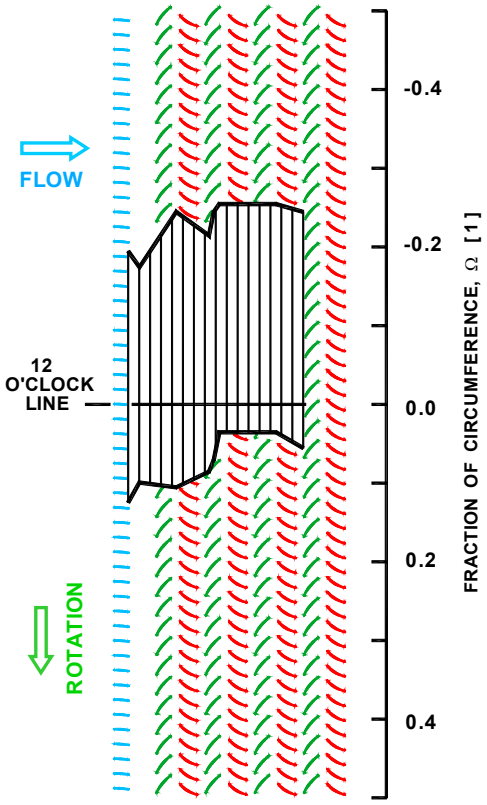

Figure 9. Detected rotating stall cell shape on the compressor shroud.

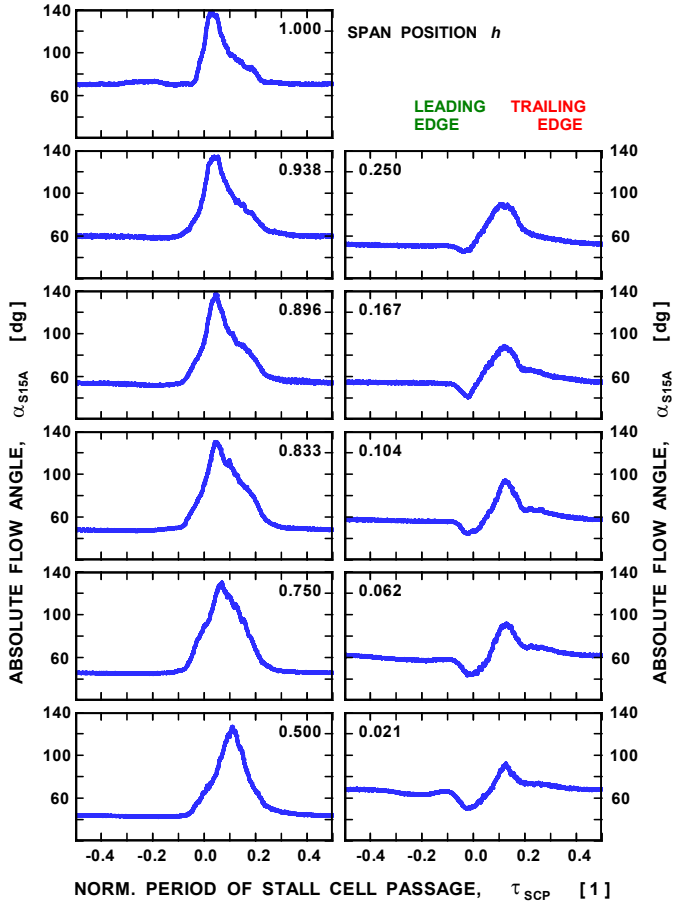

Figure 10. Distributions of absolute flow angles in a rotating stall cell along the blade height behind the first rotor (port S15A).

presents results of many repetitive test runs, over a period of several months, with all probes available, giving a good indication of high repeatability and reliability of the results presented. Measurement uncertainties and standard deviations of ensemble averaged data are discussed in detail in Ref. 9. In short, typical standard deviations of pressure measurements in terms of pressure coefficient C_{PS} were *0.04* for the unstalled portion of the flow and *0.11* for the stall cell region.

It was not obvious how to determine exactly the stall cell boundaries, in particular for the measurement stations ahead of the first rotor (stations *S05A* and *S10B*); therefore it was decided, somewhat arbitrarily, to define the leading and trailing boundaries of the stall cell by the phases at which the absolute value of pressure distribution slope changed by a factor of two. Using this loose criterion, the width of the rotating stall cell was determined at each measurement station, and was plotted in Fig. 9 superimposed over the compressor blading. The rotating stall cell traverses the entire compressor, largely in the axial direction. The progression of the stall cell through the LSAC is consistent with the active stall cell type of Ref. 4. Of course, the stall cell does not end at the fourth stage, but merely there are no available unsteady data for the last stage.

Stall Cell Spanwise Distributions

Spanwise distributions of the instantaneous absolute flow angle, axial and tangential velocity components, and static pressure data were acquired behind the first rotor (at stations *S15A* and *S15B*), behind the third rotor (stations *S35A* and *S35B*), and in front of the fourth rotor (stations *S40A* and *S40B*). The spanwise data from the third and forth rotor have not been reduced yet, so only data from behind the first rotor will be presented here.

Distributions of flow angle, axial and tangential velocity components, and flow static pressures at eleven stations along the blade span are presented in Figs. 10 through 13, respectively. As seen in Fig. 10, the absolute flow angle inside the rotating stall cell reaches *130 dg* in the outer half of the flow annulus (mid-span to case), but only *90 dg* in the inner half (mid-span to hub). This is indicative of a reversed flow (stalled) region in the outer annulus, whereas the flow does not reverse (axially) in the inner half of span. The standard deviations of angle measurements were *2 dg* in the unstalled flow and *21 dg* in the stall cell.

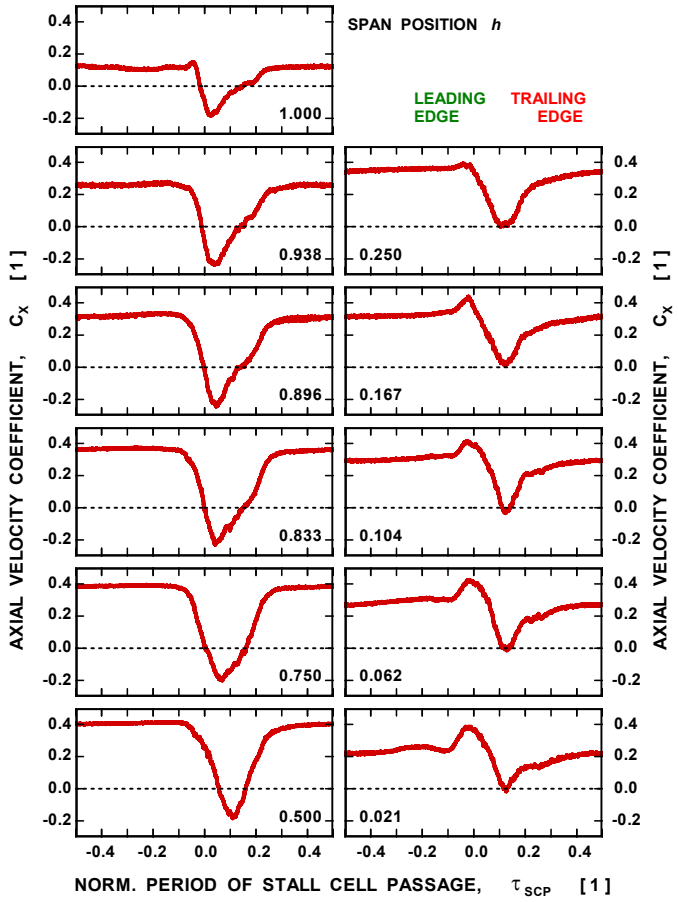

Figure 11. Distribution of axial velocity component in a rotating stall cell along the blade height behind the first rotor (port S15A).

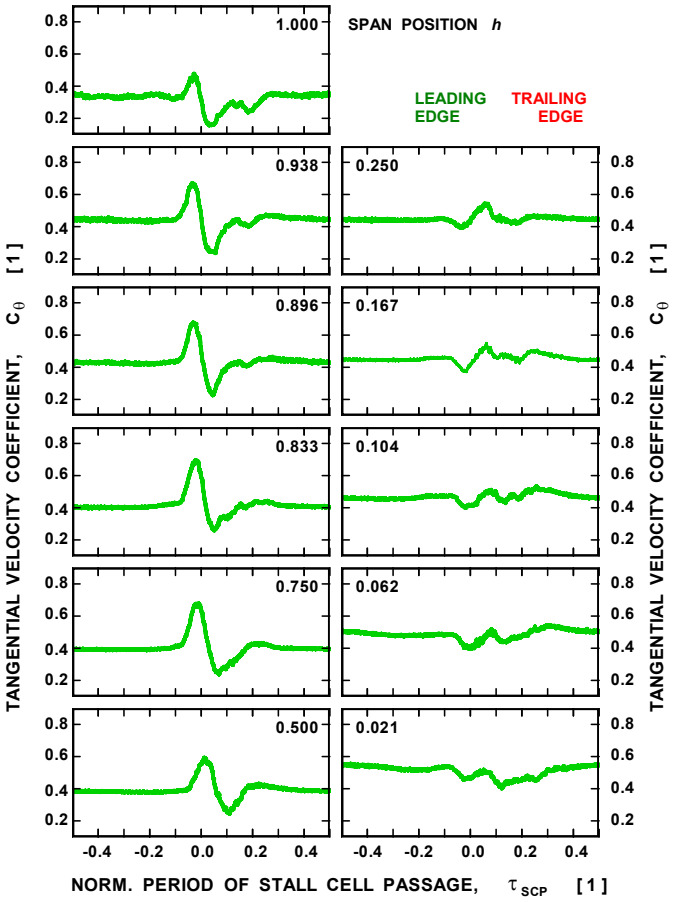

Figure 12. Distribution of tangential velocity in a rotating stall cell along the blade height behind the first rotor (port S15A).

As seen in Fig. 11, the axial velocity reverse (axially) in the inner half of span. The axial velocity component, consistent with the flow angle, exhibits a severe depression to negative values inside the rotating stall cell, but reverses to negative values only in the outer annulus (mid-span to case). At inner radii, the axial velocity first increases slightly at the leading edge of the rotating stall cell, and than drops momentarily to zero. The tangential velocity (Fig. 12) increases significantly at the rotating stall leading edge (up to *75%* of the free stream value). The tangential velocity rapidly drops to a level below that in the unstalled region, and then finally returns to the unstalled flow level. This flow pattern is restricted to the outer flow annulus, whereas in the inner half the tangential velocity is affected very little by the passage of the rotating stall cell. The standard deviations of ensemble averaged velocity data were in terms of both velocity coefficients *0.02* for the unstalled flow and *0.16* for the stall cell region. The last figure in this group, Fig. 13, depicts the distribution of flow static pressures. Again, even here the differences between upper and lower halves of the blade channel can be detected, albeit not as pronounced as in the previous cases. The main difference is a drop in the static pressure at the stall cell leading edge in the outer annulus half, which is absent in the inner part of the flow annulus.

The distributions of unsteady flow parameters, presented above, are summarized in the contour plots of Fig. 14 in order to give an overall view of the phase-locked flow field during rotating stall cell from measurement station *S15A*. The flow angle, axial velocity component, tangential velocity component, and flow static pressure are presented in the contour plots together with a properly scaled rotor and stator blade rows.

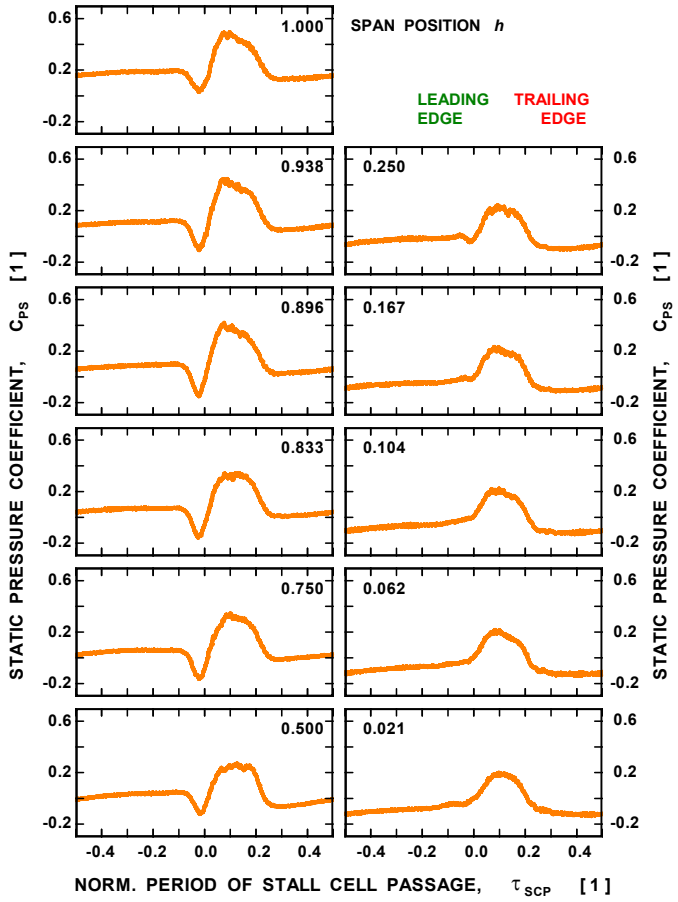

Figure 13. Distribution of static pressure in a rotating stall cell along the blade height behind the first rotor (port S15A).

The spanwise variation in all four parameters is indicative of different patterns between the inner and outer blade span regions. The flow angle and axial velocity contour fields exhibit very similar overall patterns. Within the stall cell region ($0 < \tau_{scp} < 0.2$), the highest flow angles (*125 dg*) and most negative values of axial velocity coefficient (*-0.2*) are in the blade tip region. Moving down the blade span, the maximum flow angle gradually decreases to the tangential direction (*90 dg*), and the minimum axial velocity increases to a zero value close to the compressor hub. As seen in the next contour plot, the tangential velocity component significantly increases at the stall cell leading edge, which is followed by a quick depression. The changes in the tangential velocity in the inner half of the flow annulus are much less dramatic. Finally, the flow static pressure pattern is somewhat reversed to the pattern of tangential velocity; there is a rapid static pressure drop at the cell leading edge and subsequent fast increase in pressure level across the width of the rotating stall cell.

Finally, vector plots of flowfields at the blade tip, blade midspan, and the blade root were created in order to visualize the changes among the three flow patterns in the axial-tangential plane. These plots are presented in Fig. 15. It should be realized that the vector plots for each span station depict time-resolved measurements obtained at a fixed point. The spatial separation of individual velocity vectors represents the sequence of velocity vector changes in time at a given fixed point of measurement. A similar vector plot at the blade midspan height based on an older set of data was previously presented in Ref. 9, however with an erroneously scaled picture of the rotor blade row.

Transients Into Rotating Stall

Although this paper is focused mainly on measurements in the developed rotating stall, several observations on the onset of rotating stall regime are summarized here. The same procedure for inducing the rotating stall was used throughout the investigation. As mentioned earlier, the compressor was first throttled to the near-stall operating point ($\Phi = 0.35$) and allowed to equilibrate. The throttle valve was then closed at its maximum rate, and once the rotating stall was detected, the valve motion was stopped and immediately reversed. The entire procedure lasted from *6 s* to *8 s* as depicted in Fig. 5.

In about *90%* of the cases observed, the rotating stall started with a single cell, creating the response at measurement station *S05A* provided in Figs. 4 and 16. Once the stall cell appeared, it intensified rapidly into a fully developed state. This maturation from an emerging stall cell to a fully-developed (quasi-static) stall cell occurred within four rotations of a stall cell, or eight rotor revolutions (slightly over a half of a second). No substantial change in the circumferential extent and rotational speed of the rotating stall cell was observed during the maturation period.

On occasion, the rotating stall regime started with two emerging stall cells as shown in Fig. 17. The root cause of the variable stall-cell-number is unknown. The compressor operating condition and the throttling procedure are considered highly repeatable; therefore, the variations in stall cell count are not attributed to changes in operation. As seen in the three examples of Fig. 17, one of the emerging pair of stall cells always intensified faster than the other, and quickly became the dominant (and ultimately the solely detectable) stall cell. In all of the two-stall-cell cases observed, the rotational speed of both cells was *60.7%* of the rotor speed, about *20%* higher than the ultimate speed of the single stall cell. During the short period of two cells presence, the cells were not distributed uniformly around the circumference, and no relative motion, cell merging nor splitting was observed.

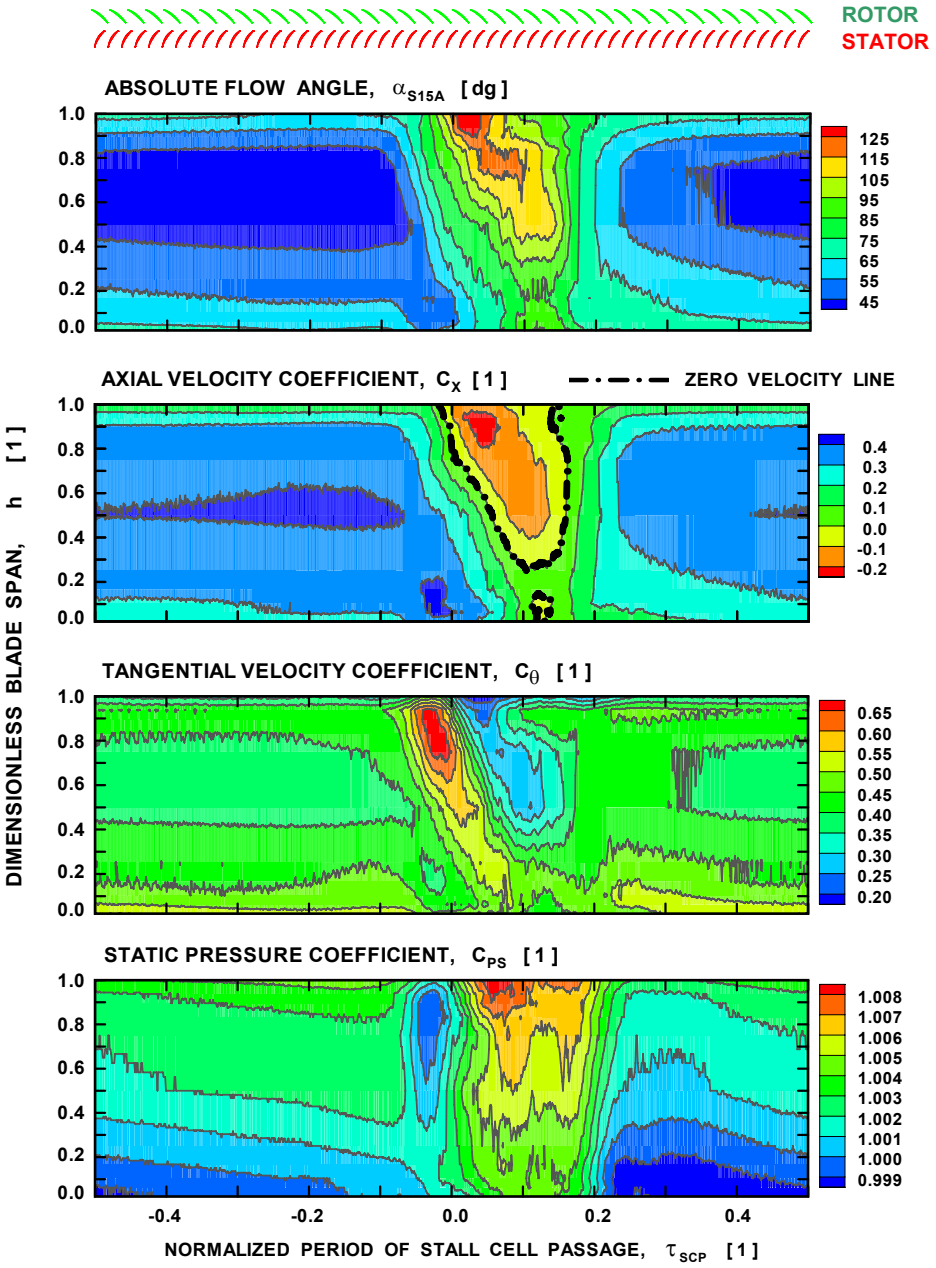

Figure 14. Contour plots of flow parameters in radial-tangential plane behind the first stage rotor for rotating stall regime.

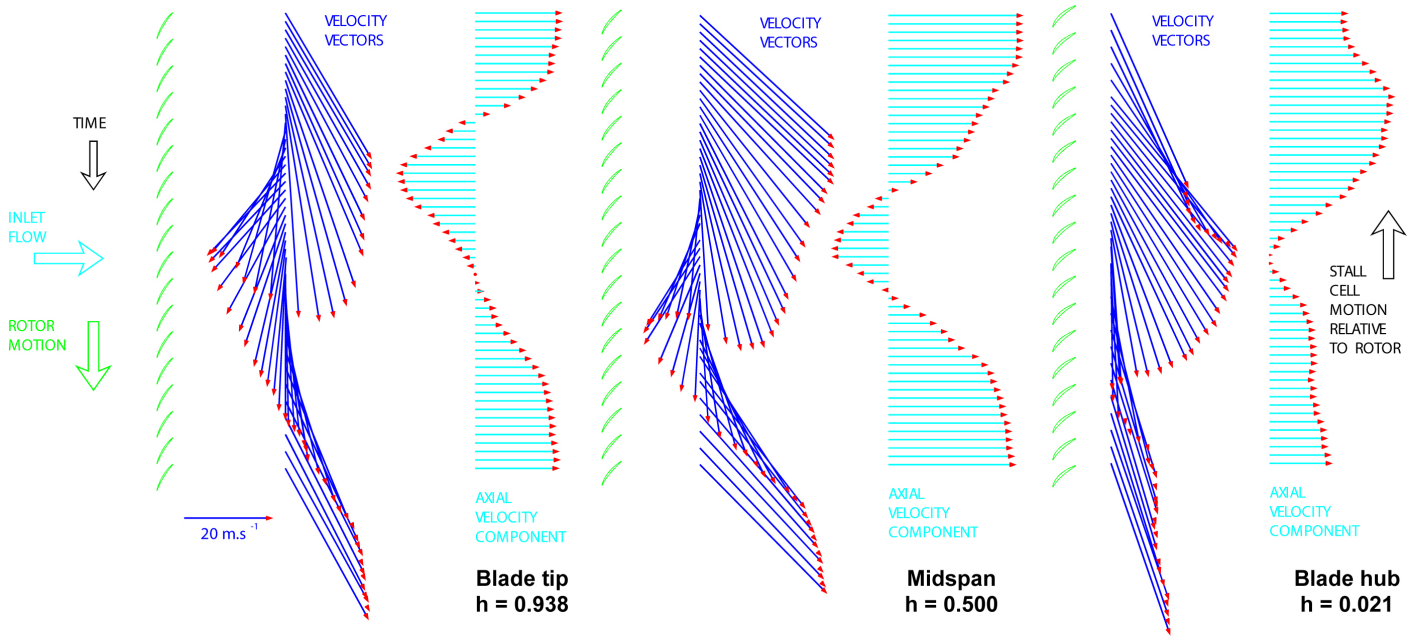

Figure 15. Flow patterns of rotating stall in axial-tangential plane behind the first stage rotor measured at three span stations (blade tip, midspan, and blade hub).

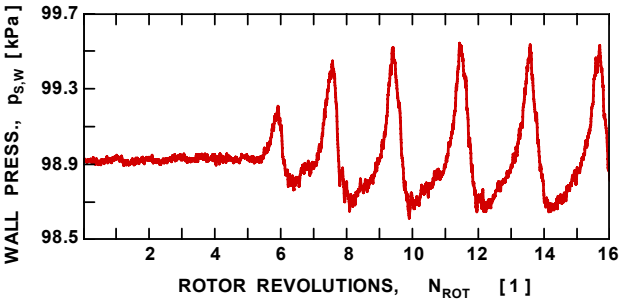

Figure 16. Transient to rotating stall regime starting with a single stall cell.

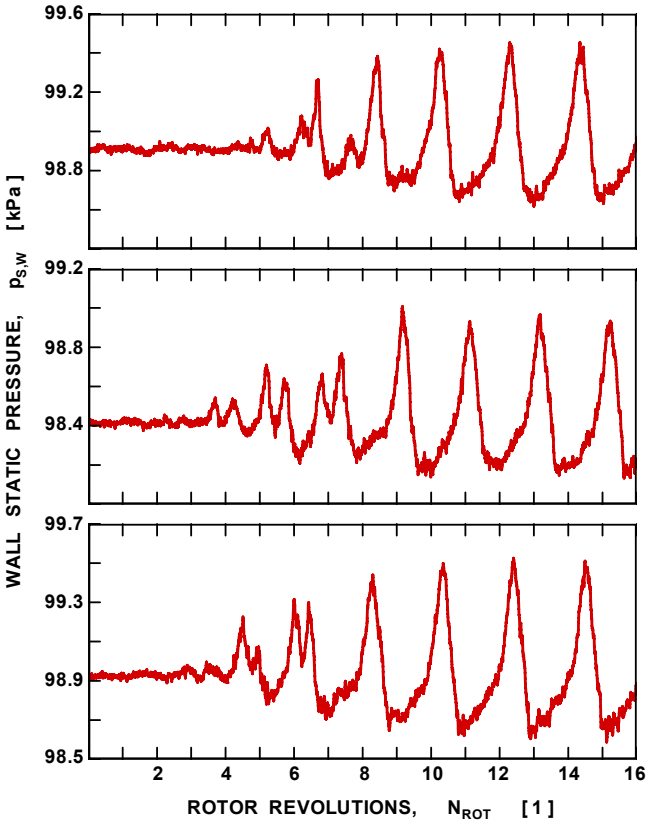

Figure 17. Transients to rotating stall starting with two stall cells.

Summary

Data and findings derived from experiments in the NASA low-speed multistage (4.5-stage) axial compressor while in fully developed rotating stall were reported herein. Unsteady casing static pressure traces from various circumferential and axial position within the compressor indicate that a single fully developed stall cell extended axially through the machine and rotated about the flow annulus at *50.6%* of the rotor speed.

Full-span surveys showed strong spanwise variation in the ensemble averaged static pressure, axial and tangential velocities, and flow angle obtained during stall. The flow within the stall cell is axially reversed flow from mid-span to the casing, whereas the flow from the hub to mid-span was not reversed axially, although significantly reduced.

The time-traces from instantaneous casing statics ahead of the first rotor during stall inception induced by a repeatable, rapid throttling of the flow typically indicated an emerging single stall cell traveling at *50.6%* of the rotor speed, which intensified as it matured into fully developed cell. On some occasions however, two emerging stall cells traveling at *60.7%* of the rotor speed were noted; consistently, one of the two emerging stall cells would decay while the other intensified into a fully developed stall cell traveling at *50.6%* of the rotor speed.

References

1. Emmons, H.W., Pearson, C.E., and Grant, H.P.: "Compressor Surge and Stall Propagation," *Transactions of the ASME*, vol. 77, pp. 455–469, 1955.
2. Greitzer, E.M.: "Surge and Rotating Stall in Axial Flow Compressors, Part II," *ASME Journal of Engineering for Power*, vol. 98, pp. 199–217, 1976.
3. Day, I.J., Greitzer, E.M., and Cumpsty, N.A.: "Prediction of Compressor Performance in Rotating Stall," *ASME Journal of Engineering for Power*, vol. 100 pp. 1–14, 1978.
4. Day, I.J. and Cumpsty, N.A.: "The Measurement and Interpretation of Flow within Rotating Stall Cells in Axial Compressors," *Journal of Mechanical Engineering Science*, vol. 20, no. 2, pp. 101–114, 1978.
5. Das, D.K. and Jiang, H.K.: "An Experimental Study of Rotating Stall in a Multistage Axial-Flow Compressor," *ASME Journal of Turbomachinery*, vol. 106, pp. 542–551, 1984.
6. McDougall, N.M., Cumpsty, N.A., and Hynes, T.P.: "Stall Inception in Axial Compressors," *ASME Journal of Turbomachinery*, vol. 112, pp. 116–125, 1990.
7. Camp, T.R. and Day, I.J.: "A Study of Spike and Modal Stall Phenomenon in a Low-Speed Axial Compressor," *ASME Journal of Turbomachinery*, vol. 120, pp. 393–401, 1998.
8. Nie, C., Chen, J., Jiang, H., and Xu, L.: "Experimental analysis on the unsteady behavior of modal stall inception in a low-speed axial compressor," Paper ISABE 99–7218, 1999.
9. Lepicovsky, J. and Braunscheidel, E.P.: "Measurement of Flow Pattern Within a Rotating Stall Cell in an Axial Compressor," NASA/TM—2006-214270, 2006.
10. Wasserbauer, C.A., Weaver, H.F., and Senyitko, R.G.: "NASA Low-Speed Axial Compressor for Fundamental Research," NASA TM–4653, 1995.
11. Wellborn, S.R. and Okiishi, T.H.: "Effects of Shrouded Stator Cavity Flows on Multistage Axial Compressor Aerodynamic Performance," NASA CR–198536, 1996.
12. Lepicovsky, J.: "Unsteady Velocity Measurements in the NASA Research Low Speed Axial Compressor," NASA CR–214815, 2007.
13. Wisler, D.C.: "Core Compressor Exit Stage Study," NASA CR–135391, 1977.
14. Lepicovsky, J. "Application of a Split-Fiber Probe to Velocity Measurement in the NASA Research Compressor," NASA CR–212489, 2003.
15. Lepicovsky, J. "Measurements With a Split-Fiber Probe in Complex Unsteady Flows," NASA CR–213065, 2004.

REPORT DOCUMENTATION PAGE	Form Approved OMB No. 0704-0188

1. REPORT DATE *(DD-MM-YYYY)*	2. REPORT TYPE	3. DATES COVERED *(From - To)*
01-08-2007	Technical Memorandum	

4. TITLE AND SUBTITLE
Experimental Investigation of Rotating Stall in a Research Multistage Axial Compressor

5a. CONTRACT NUMBER

5b. GRANT NUMBER

5c. PROGRAM ELEMENT NUMBER

6. AUTHOR(S)
Lepicovsky, Jan; Braunscheidel, Edward, P.; Welch, Gerard, E.

5d. PROJECT NUMBER

5e. TASK NUMBER

5f. WORK UNIT NUMBER
WBS 561581.02.08.03.21.02

7. PERFORMING ORGANIZATION NAME(S) AND ADDRESS(ES)
National Aeronautics and Space Administration
John H. Glenn Research Center at Lewis Field
Cleveland, Ohio 44135-3191

8. PERFORMING ORGANIZATION REPORT NUMBER
E-16134

9. SPONSORING/MONITORING AGENCY NAME(S) AND ADDRESS(ES)
National Aeronautics and Space Administration
Washington, DC 20546-0001
and
U.S. Army Research Laboratory
Adelphi, Maryland 20783-1145

10. SPONSORING/MONITORS ACRONYM(S)
NASA, ARL

11. SPONSORING/MONITORING REPORT NUMBER
NASA/TM-2007-214978; ARL-TR-4126

12. DISTRIBUTION/AVAILABILITY STATEMENT
Unclassified-Unlimited
Subject Categories: 07 and 09
Available electronically at http://gltrs.grc.nasa.gov
This publication is available from the NASA Center for AeroSpace Information, 301-621-0390

13. SUPPLEMENTARY NOTES

14. ABSTRACT
A collection of experimental data acquired in the NASA low-speed multistage axial compressor while operated in rotating stall is presented in this paper. The compressor was instrumented with high-response wall pressure modules and a static pressure disc probe for in-flow measurement, and a split-fiber probe for simultaneous measurements of velocity magnitude and flow direction. The data acquired to-date have indicated that a single fully developed stall cell rotates about the flow annulus at 50.6% of the rotor speed. The stall phenomenon is substantially periodic at a fixed frequency of 8.29 Hz. It was determined that the rotating stall cell extends throughout the entire compressor, primarily in the axial direction. Spanwise distributions of the instantaneous absolute flow angle, axial and tangential velocity components, and static pressure acquired behind the first rotor are presented in the form of contour plots to visualize different patterns in the outer (mid-span to casing) and inner (hub to mid-span) flow annuli during rotating stall. In most of the cases observed, the rotating stall started with a single cell. On occasion, rotating stall started with two emerging stall cells. The root cause of the variable stall cell count is unknown, but is not attributed to operating procedures.

15. SUBJECT TERMS
Unsteady flow; Compressors; Velocity measurements

16. SECURITY CLASSIFICATION OF:			17. LIMITATION OF ABSTRACT	18. NUMBER OF PAGES	19a. NAME OF RESPONSIBLE PERSON
a. REPORT	b. ABSTRACT	c. THIS PAGE			STI Help Desk
U	U	U		16	19b. TELEPHONE NUMBER *(include area code)*
					301-621-0390